

## Dynamic Observation of an Atom-Sized Gold Wire by Phase Electron Microscopy

Yoshizo Takai,<sup>1,\*</sup> Tadahiro Kawasaki,<sup>1</sup> Yoshihide Kimura,<sup>1</sup> Takashi Ikuta,<sup>2</sup> and Ryuichi Shimizu<sup>3</sup>

<sup>1</sup>*Department of Material and Life Science, Graduate School of Engineering, Osaka University,  
2-1 Yamada-oka, Suita, Osaka 565-0879, Japan*

<sup>2</sup>*Department of Lightwave Science, Osaka Electro-Communication University,  
Neyagawa, Osaka 572-8530, Japan*

<sup>3</sup>*Department of Information Processing, Osaka Institute of Technology,  
Kitayama 1-79-1, Hirakata, Osaka 573-0196, Japan*

(Received 1 February 2001; published 21 August 2001)

A single-atom-sized gold wire was successfully observed in real time by a newly developed defocus-image modulation processing electron microscope. Because of phase retrieval processing with spherical aberration correction, the single-atom strand wire was observed with high contrast and without contrast blurring. By carefully looking at the atomic distance, the contrast, and the dynamic behavior of the wire, we recognized that there are two stages of the wire. In the first stage the wire maintained the atomic distance in the bulk crystal, but in the second stage the wire showed the atomic distance of the nearest-neighbor atoms with weaker contrast. The gold wire was rather stable for a few seconds under strong electron beam illumination.

DOI: 10.1103/PhysRevLett.87.106105

PACS numbers: 68.65.La, 07.78.+s, 42.30.Rx, 68.37.Lp

Atom-sized wires have recently received a great deal of attention as an ideal one-dimensional material having quantized conductance in steps of  $2e^2/h$ , where  $e$  is the electron charge and  $h$  is Planck's constant. In terms of theoretical physics and electronic applications using quantum effects, it is very important to examine the detailed relationship between an electronic property and its atomic structure. Ohnishi *et al.* [1] attempted to confirm such a relationship on an atomic scale by constructing a scanning tunneling microscope (STM) in an ultrahigh vacuum transmission electron microscope (TEM). In their experiments, they made an atom-sized gold wire by drawing a gold STM tip from a gold substrate, then confirmed quantized conductance in steps of  $2e^2/h$  while using the TEM to observe the wire on an atomic scale. In the TEM image, they found an unusually long atomic spacing of about 0.4 nm in the atom-sized gold wire that is elongated along the [001] direction. The electronic property of a gold wire with an abnormal atomic spacing is very interesting in terms of quantum electronics. Although many researchers have been trying to explain this abnormal atomic spacing using approaches based on computational physics, none have succeeded. In their images, extra interference fringes, caused by the influence of the lack of focus and the remaining spherical aberration, appear outside the crystal region. Such fringes prevent the precise observation of the atomic structure of the wire.

Because spherical aberration-free phase imaging has a high potential for providing direct determination of localized atomic structures, many methods have been proposed thus far by hardware and software techniques [2–5]. As one of the most promising approaches, we propose the use of defocus-image modulation processing (DIMP) [6–9]. In this process, integration of defocus images multiplied by specific weights is performed to produce a spherical

aberration-free phase image, as is described in detail elsewhere [10]. To develop this real-time processing, a research project called the “Development of a Next-Generation Super Electron Microscope” was started in 1996 under the support of the Japan Society for Promotion of Science (JSPS). In our most recent papers [11–13], we reported that a real-time defocus-image modulation processing electron microscope (DIMP-EM) was successfully developed as one of the next-generation electron microscopes, using a 200 kV field emission TEM (HF-2000F) as a platform apparatus. This microscope enabled the observation of spherical aberration-free phase images with a time resolution of 4/30ths of a second. In the real-time DIMP-EM, focus is controlled by modulating the accelerating voltage using a custom-designed, floating-type, high-voltage generation system to achieve rapid and precise control of focusing. The integration of weighted images, which is an indispensable procedure for DIMP operation, is performed in an image recording camera by controlling the focus every 8  $\mu$ s within the period of a single video frame (1/30th of a second) [12]. Because both spherical aberration correction and phase retrieval processing occur simultaneously, superhigh-resolution phase electron microscopy is achieved. As an application of the real-time DIMP-EM, the movement of surface atoms on a reconstructed Au (011) surface was reported in a previous paper [13]. In the present paper, the real-time DIMP-EM is further applied to the observation of an atom-sized gold wire.

Figure 1 is a series of images of a gold wire observed by the real-time DIMP-EM. These images were reproduced from video images that are processed at a time resolution of 4/30ths of a second. In a conventional high-resolution TEM image of such a crystal edge area, some extra lattice fringes usually appear outside the crystal region. However, no such fringes appear in these phase electron microscope

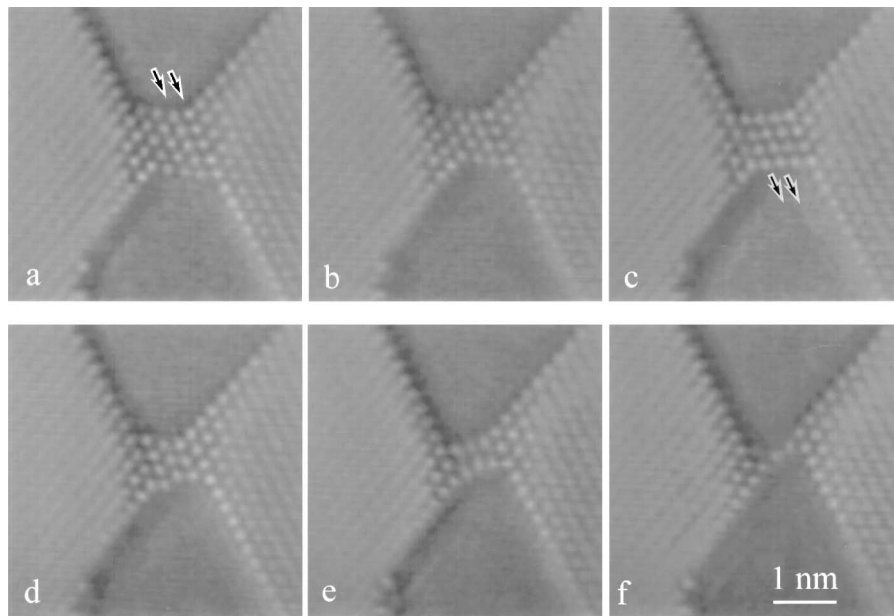


FIG. 1. Dynamic observation of spherical aberration-free phase image of gold wire: (a) 0.00 s, (b) 0.80 s, (c) 0.93 s, (d) 3.20 s, (e) 7.20 s, and (f) 7.73 s.

images because of the spherical aberration correction. The surface atoms on the crystal edge can be clearly observed in a profile image mode by the real-time DIMP-EM. In the phase image, a high-contrast white dot appears even in very thin regions. Conversely, the contrast becomes rather low in thick regions. This is because the phase information is lost due to the effect of dynamic electron diffraction in thick areas.

The series of images show how the wire becomes thinner and thinner under intense electron beam irradiation of  $100 \text{ A/cm}^2$  on the sample during observation. The original wire was fabricated in TEM by making two adjacent holes on a (110) gold single-crystal film using a converged electron beam. The base pressure of the microscope was  $1 \times 10^{-6} \text{ Pa}$ . The gold thin film is supported on a conventional holly carbon microgrid, and the fabricated gold wire is self-supported in the vacuum without overlapping by the supported carbon film. The sample thickness seems to be almost the same with the wire width.

In Fig. 1(a), a short wire consisting of five rows of atoms is seen very clearly in the center of the figure, where a stacking fault is formed between the atomic planes indicated by the arrows. In Fig. 1(b), the number of rows of atoms constituting the wire decreases to four due to the surface migration of the gold atoms under electron beam irradiation. A large amount of stress is produced by the relative shift between both side crystals, as is clearly seen by a bending of the horizontal (111) atomic planes at the bridging part. At 4/30ths of a second after the time of Fig. 1(b), the stress is suddenly relaxed in Fig. 1(c) by the slipping of the two (111) atomic planes indicated by the arrows, resulting in twin formation with four layers of atoms at the bridging part. Crystal deformation followed by the movement of the

stacking faults, which is caused by the stress between the two crystal regions, was also observed between Figs. 1(d) and 1(e). Finally, we observed an atom-sized gold wire, as shown in Fig. 1(f). It should be noted that the contrast of the wire image is rather strong and that the signal-to-noise ratio of the image is relatively good even when the wire consists of a very small number of atoms.

Figure 2 shows the dynamic movement of the atom-sized wire that is continuously observed in the spherical aberration-free phase imaging mode. In the images of Figs. 2(a) and 2(c), the right-hand connecting position of the wire moves down by a distance of  $1/2[110]$  as the two crystals on both sides gradually change their relative positions. The central white dot of the wire shifts to the right in Fig. 2(d) and shifts to the left in Fig. 2(e), indicating that the center atom is maintaining a normal atomic distance in the bulk crystal when the two crystals gradually separate. Therefore, the atom-sized gold wire observed in Fig. 2 might form a crystal slab consisting of a few atoms in depth, because the wire still has the characteristics of bulk gold crystal.

By carefully looking at the contrast of the atom-sized gold wire, we recognized that there are two stages of the single-strand gold wire, as shown in Fig. 3. These images are averaged for 32/30 seconds; therefore, the signal-to-noise ratio is better than that in Fig. 2. In Fig. 3(a), the distance between the white dots of the wire is almost the same as that of the crystal region. The size of the central white dot of the wire is slightly larger than that of the others. This is because the central atom vibrates more frequently with higher amplitude due to a weaker holding force than that of the side atoms attached to the bulk crystals, judging from the dynamic movement of the wire. In Fig. 3(b), the

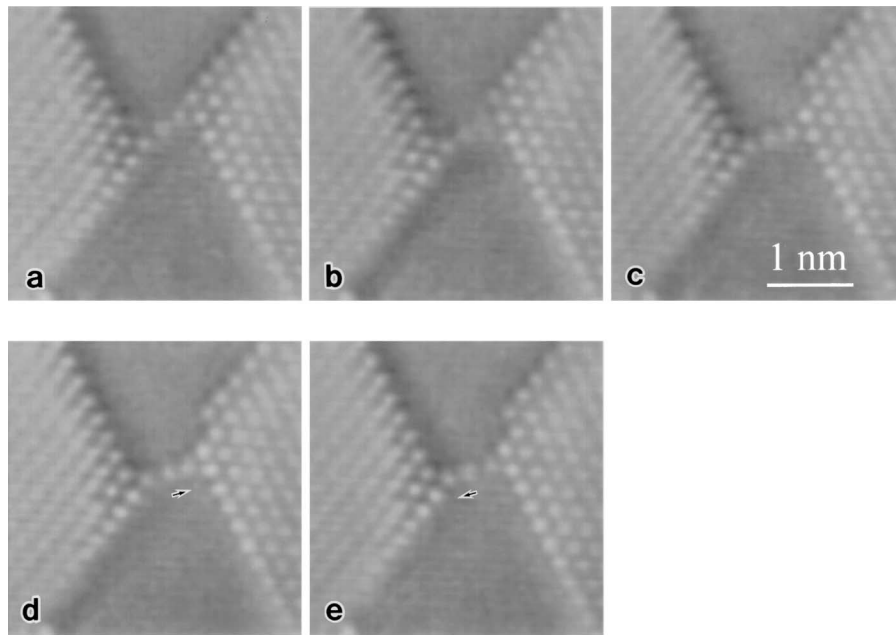


FIG. 2. Movement of atom-sized gold wire: (a) 0.00 s, (b) 0.27 s, (c) 0.40 s, (d) 0.67 s, and (e) 0.80 s.

contrast of the white dot of the wire becomes rather faint and the distance between the white dots becomes almost equal to that between the nearest-neighbor atoms. The wire in Fig. 3(b) always appeared as if it consisted of a single

row of atoms with the atomic distance of its nearest neighbor, even when the wire moved. It should also be pointed out that the single-atom-sized wire was rather stable for several seconds under strong electron beam illumination,

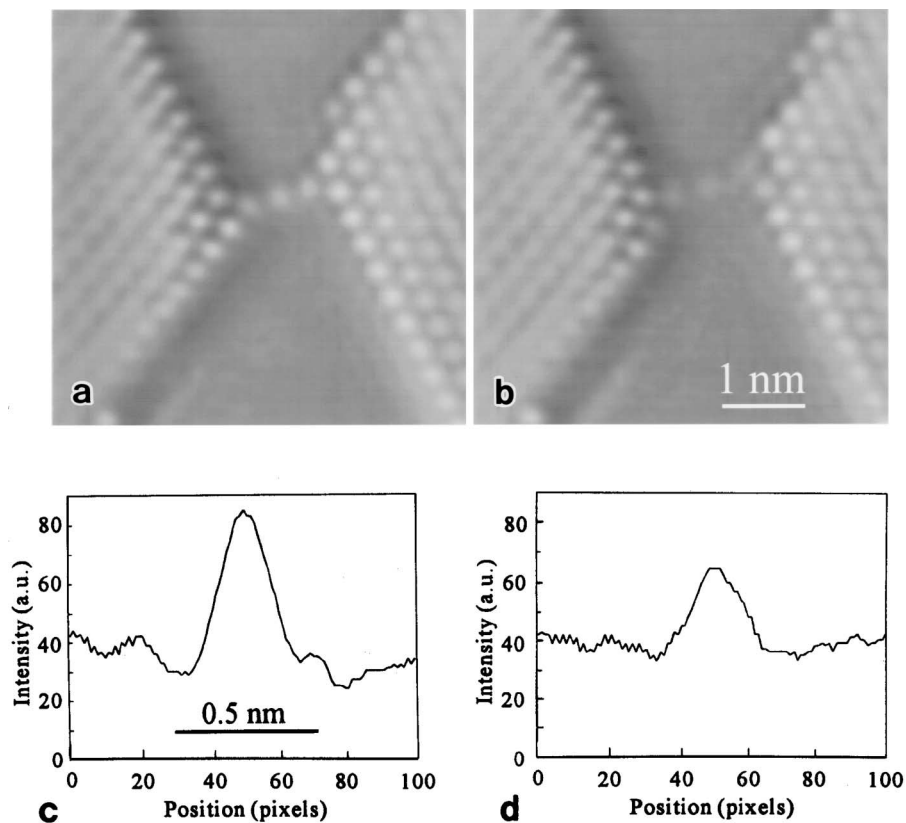


FIG. 3. Spherical aberration-free phase image of atom-sized gold wire in two stages: (a),(c) Image and intensity profile of stage I. (b),(d) Image and intensity profile of stage II.

though the wire was broken when the atomic distance became greater than that of the nearest-neighbor atoms.

Figures 3(c) and 3(d) show image intensity profiles crossing the center atom of the wire longitudinally in Figs. 3(a) and 3(b), respectively. As shown in Figs. 3(c) and 3(d), the contrast of the center atom reduced by about 1/2 within 1 s. Judging comprehensively from these experimental results, such as the observed atomic distances, the dynamic behavior of the wire, and the difference in contrast, we may conclude that the first stage of the wire in Fig. 3(a) consists of two atoms in depth and that the second stage in Fig. 3(b) is a chain of single gold atoms. The quantification of atom image contrast, size, and distances between atoms should be done very carefully even if the spherical aberration-free phase electron microscopy is achieved. However, the potential to discuss atom image contrast and determine atom positions is much improved in the proposed spherical aberration-free phase electron microscopy [14], because the phase contrast transfer function becomes flat from 1 to  $7 \text{ nm}^{-1}$  ( $= 1.4 \text{ \AA}$ ) with no oscillation in the present experiment. Furthermore, dynamic observation at an atomic level by the proposed method can give us useful evidence for understanding physical phenomena. We are now confirming, by image simulations combined with a dynamical electron diffraction theory, how precisely the phase information can be retrieved by the proposed processing.

According to the observations by Ohnishi *et al.*, the gold atoms showed a much greater atomic distance (0.4 nm) in the elongated wire along [001] direction than the nearest-neighbor atomic distance of gold crystal (0.288 nm). Although we were not able to observe the wire along the same direction, but along the [110] direction, our experiment did not show such a large atomic distance. It did show the projected atomic distance in the bulk crystal of 0.25 nm in Fig. 3(a) and the nearest-neighbor atom distance of 0.29 nm in Fig. 3(b).

High-resolution phase electron microscopy is a key means for studying atomic-scale dynamic phenomena that occur on surfaces and interfaces. A real-time DIMP-EM with a floating-type high-voltage generating system enabled us to observe phase images in real time without any spherical aberration. Dynamic observation of a single-atom-sized wire was successfully performed with high contrast at a time resolution of 4/30ths of a second.

The application of DIMP to real-time processing is very effective in enabling dynamic observation of surfaces and interfaces on an atomic scale, and might lead to a method of investigating chemical phenomena on an atomic scale. The real-time DIMP-EM may also be effective in applications requiring high-resolution observation of biological specimens. This is because spherical aberration-free phase images provide high contrast within the period of a few video frames without the need for staining, minimizing the total electron bombardment of the specimen.

This work was supported by the Japan Society for the Promotion of Science, JSPS-RFTF96R14101.

---

\*Author to whom correspondence should be addressed.

Electronic address: takai@ap.eng.osaka-u.ac.jp

- [1] H. Ohnishi, Y. Kondo, and K. Takayanagi, *Nature (London)* **395**, 780 (1998).
- [2] T. Ikuta, *J. Electron. Microsc.* **38**, 415 (1989).
- [3] D. Van Dyck and M. Op de Beck, in *Proceedings of the XIIth International Congress on Electron Microscopy* (San Francisco Press, San Francisco, 1990), Vol. 1, p. 26.
- [4] H. Lichte, E. Volkl, and K. Scherschmidt, *Ultramicroscopy* **47**, 231 (1992).
- [5] J. Zach and M. Haider, *Nucl. Instrum. Methods Phys. Res., Sect. A* **363**, 316 (1995).
- [6] Y. Taniguchi, Y. Takai, T. Ikuta, and R. Shimizu, *J. Electron. Microsc.* **41**, 21 (1992).
- [7] Y. Taniguchi, Y. Takai, R. Shimizu, T. Ikuta, S. Isakozawa, and T. Hashimoto, *Ultramicroscopy* **41**, 323 (1992).
- [8] T. Ando, Y. Taniguchi, Y. Takai, Y. Kimura, R. Shimizu, and T. Ikuta, *Ultramicroscopy* **54**, 261 (1994).
- [9] T. Ando, H. Utsuro, Y. Kimura, Y. Takai, and R. Shimizu, *Optik (Stuttgart)* **106**, 147 (1997).
- [10] Y. Taniguchi, T. Ikuta, and R. Shimizu, *Optik (Stuttgart)* **96**, 129 (1994).
- [11] Y. Takai, H. Utsuro, Y. Kimura, T. Ikuta, and R. Shimizu, *J. Electron. Microsc.* **47**, 419 (1999).
- [12] Y. Kimura, Y. Takai, T. Kawasaki, R. Shimizu, T. Ikuta, S. Isakozawa, Y. Sato, and M. Ichihashi, *J. Electron. Microsc.* **48**, 873 (1999).
- [13] Y. Takai, Y. Kimura, T. Ikuta, R. Shimizu, Y. Sato, S. Isakozawa, and M. Ichihashi, *J. Electron. Microsc.* **48**, 879 (1999).
- [14] Y. Takai, Y. Taniguchi, T. Ikuta, and R. Shimizu, *Ultramicroscopy* **54**, 250 (1994).